JACS
JOURNAL OF THE AMERICAN CHEMICAL SOCIETY
Communication
pubs.acs.org/JACS

Photoemission Mechanism of Water-Soluble Silver Nanoclusters: Ligand-to-Metal−Metal Charge Transfer vs Strong Coupling between Surface Plasmon and Emitters

Yuting Chen,[†,§] Taiqun Yang,[†,‡,§] Haifeng Pan,[†] Yufeng Yuan,[†] Li Chen,[‡] Mengwei Liu,[†] Kun Zhang,*[,‡] Sanjun Zhang,*[,†] Peng Wu,[‡] and Jianhua Xu[†]

[†]State Key Laboratory of Precision Spectroscopy and [‡]Shanghai Key Laboratory of Green Chemistry and Chemical Processes, Department of Chemistry, East China Normal University, Shanghai 200062, P. R. China

Supporting Information

ABSTRACT: Using carboxylate-protected silver nanoclusters (Ag-carboxylate NCs) as a model, we separately investigated the contribution of the ligand shell and the metal core to understand the nature of photoluminescence of Ag NCs. A new Ag(0)NCs@Ag(I)-carboxylate complex core−shell structural model has been proposed. The emission from the Ag-carboxylate NCs could be attributed to ligand-to-metal−metal charge transfer from Ag(I)-carboxylate complexes (the oxygen atom in the carboxylate ligands to the Ag(I) ions) to the Ag atoms and subsequent radiative relaxation. Additionally, we found that the emission wavelength of the Ag NCs depends on the excitation wavelength implying a strong coupling between surface plasmon and emitter in Ag NCs. The strong coupling between the surface plasmon and the emitter determines the quantum yield and lifetime. The emission mechanism of Ag NCs and its relation to the organic templates and metal cores were clearly clarified. The results should stimulate additional experimental and theoretical research on the molecular-level design of luminescent metal probes for optoelectronics and other applications.

Metal nanoclusters (NCs) with size approaching the Fermi-wavelength of an electron (<1 nm) and exhibiting molecular-like characteristics have been very actively investigated in a variety of fields including chemistry, medicine, and biology. Au and Ag NCs in particular have attracted tremendous interest because of their wide applications in single-molecule studies, sensing, biolabeling, catalysis, and biological fluorescence imaging.[1−6] However, the mechanism of photoemission from metal NCs remains unclear.

The optical properties of metal nanostructures strongly depend on their size. Surface plasmon resonance is the dominant effect in large metal nanostructures from tens to hundreds of nanometers.[7] As their size is reduced to the Fermi wavelength of metals (usually <1 nm), the continuous state density becomes discrete due to quantum confinements. Fluorescent Ag NCs with only 7−9 Ag atoms and size <1 nm have been reported.[8] In theory, only metal NCs with sizes <2 nm could exhibit photoemission due to intrinsic states quantization effects. However, photoemission has also been observed in larger NCs in the range of 2−5 nm[9−14] and even as large as 18 nm.[15] These observations suggest that the photoemission mechanism from metal NCs cannot be simply attributed to the small size and quantization effects. In fact, the size of many fluorescent Au and Ag NCs commonly prepared by wet chemical synthesis is in this exact size range (2−5 nm). The small size and unknown surface or interfacial structure have made it difficult to deeply evaluate the contribution of each part to the fluorescence signal in the 2−5 nm class of nanoparticles.

Recently, two independent and prominent studies were carried out to investigate the photoemission mechanism of Au-thiolate NCs. In their proposed core−shell structure model, several typical and common characteristics of NCs were observed including high selectivity of the anchoring thiolate ligands and high surface charge state.[16,17] These interesting experimental observations confirmed that both the anchoring ligands and the surface charge on the NC core are pivotal to the control of photoemission. Fluorescent Ag NCs have been prepared with various scaffolds such as carboxylate groups ($-COO^-$)[9−12,18−21] and DNAs.[13,22−27] The photoemission from Ag NCs was usually attributed to the small size controlled by the scaffolds,and the contributions of the anchoring ligand were rarely considered. However, these seemingly unrelated but very important experimental phenomena suggest the common nature of noble metal NCs photoemission.

Herein, 2−5 nm water-soluble fluorescent Ag-carboxylate NCs were synthesized by the soft UV photoreduction strategy, using polyelectrolyte poly(methacrylic acid) (PMAA) as a scaffold and were characterized with fluorescence spectroscopy. Versus conventional wet chemical synthesis using strong reducing agent such as sodium borohydride ($NaBH_4$), the mild photoreduction protocol offers an alternative to precisely tune the size of the NCs. Using carefully controlled experimental conditions, we first proposed that the origin of photoemission of Ag-carboxylate NCs is ligand-to-metal−metal charge transfer (LMMCT) from Ag(I)-carboxylate complexes. That is, the photoemission of Ag(I)-carboxylate Ag NCs arises from electron transfer from the oxygen atom in the carboxylate ligands to the Ag(I) ions to the Ag atoms and subsequent radiative relaxation. The luminescence intensity and color depend on the nanoparticle size and the excitation wavelengths.

Received: July 31, 2013
Published: January 17, 2014

dx.doi.org/10.1021/ja407911b | J. Am. Chem. Soc. 2014, 136, 1686−1689

The polyelectrolyte PMAA was used as the model carboxylate ligand for the synthesis of Ag-carboxylate NCs similar to previous reports.[19] A freshly prepared mixture solution of PMAA (0.8 M, 6 mL) and $AgNO_3$ (0.05 M, 24 mL) was incubated in the dark for ~10 min and then exposed to UV irradiation at 365 nm for various times. The characterization by UV−vis absorption and photoluminescence spectroscopy clearly showed that the highly fluorescent AgNCs were synthesized using one-step aqueous photoreduction in the presence of multidentate ligands made of PMAA anchoring groups. The evolution of the absorption spectra at various times is shown in Figure 1a.

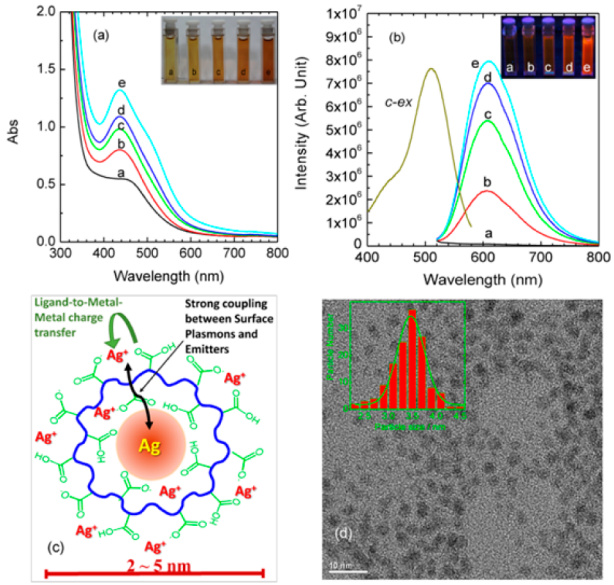

Figure 1. (a) UV−vis absorption of the freshly prepared Ag-carboxylate NCs using PMAA as scaffold at various radiation times (a, 0 min; b, 10 min; c, 20 min; d, 30 min; and e, 40 min.) (b) PL spectra of the Ag-carboxylate NCs. Inset images show the corresponding photographs of Ag-carboxylate NCs under room and UV light exposure at λ = 365 nm. Fluorescence spectra were measured at λ_{ex} = 505 nm. The curve c-ex is the excitation spectrum of sample c. (c) Schematic illustration of the structures of our luminescent Ag-carboxylate with Ag^+-carboxylate complexes shell. (d) TEM image of freshly prepared Ag-carboxylate NCs (histogram describes the statistical distribution of the particle size, which is ~3.5 nm). Images of other scales are shown in Figure s1. The COO^-/Ag^+ molar ratio used for the synthesis was 4:1.

Prior to irradiation, the solution had a broad absorption band centered at 450 nm, which is attributed to the ligand-to-metal charge transfer (LMCT) of the oxygen atom in the carboxylate ligands to the Ag(I) ions. After 10 min of UV irradiation, a strong and sharp absorption band centered at ~435 nm appeared. The intensity of this absorption band increased with increasing exposure time. Meanwhile, a shoulder peak at ~505 nm was also observed upon their radiation. Importantly, when we changed the reaction conditions such as the pH value, molar ratio of COO^-/Ag^+, and storage time, the relative absorption intensity at 435 and 505 nm can be tuned (Figures s3 and s4), but the position of the bands remained constant. It is important to note that the peak centered at 435 nm did not disappear; rather, the relative contribution at 435 nm and 505 nm decreased. These bands have been assigned to Ag NCs with different atom numbers at 435 and 505 nm.[8,9,19] If this were true, then when the reaction conditions changed, the number of Ag atoms in NCs should change, resulting in different bands, not just those located at 435 and 505 nm. We instead suggest that the two adsorption bands come from the plasmonic resonance and LMMCT in Ag NCs, respectively.

The TEM observations in Figures 1d and s1 show that the ultrasmall and homogeneous NCs with an average diameter of 3.5 nm were formed when the UV irradiation time was 20 min. Although the Ag NCs appear monodisperse in solution from TEM, the Ag NCs are actually formed within the PMAA macromolecules, as confirmed by the coupled atomic force imaging (AFM) and confocal imaging (Figure s5). The PMAA polymer formed patch and thread-like structures at high and low Ag NC concentrations, respectively. The similarity between confocal fluorescence and AFM images proved that fluorescence comes from the Ag(0)NCs@Ag(I)-carboxylate complex, i.e., the 3.5 nm Ag NCs. The possibility that the fluorescence originates from byproducts of Ag NC solution was ruled out.

According to quantum confinement theory, Ag NCs with a size larger than 2 nm are too large to produce fluorescence. However, strong luminescence was observed upon excitation (inset of Figure 1b). The initial solution exhibited no visible emission prior to UV radiation, but after a 10 min irradiation at 365 nm an intense emission band centered at 600 nm was observed. The emission intensity increased monotonically with increasing irradiation time. The quantum yield (QY) of as-made Ag-carboxylate NCs was measured to be ~4.6% using Rhodamine B in ethanol as the reference. As demonstrated in Figure s6, the time-resolved fluorescence measurements indicate that the average lifetime is ~1 ns, and the predominant lifetime is in 100−200 ps range in the Ag-carboxylate NCs [0.13 ns (63%), 0.69 ns (31%), and 1.61 ns (6%) upon excitation at 430 nm; 0.10 ns (55%), 0.60 ns (32%), and 1.57 ns (13%) upon excitation at 505 nm (Table s1)]. The lifetime is almost the same for the Ag NCs with different UV radiation times (Table s1). This suggests that the energy level structure of the fluorophore does not change, only the amount of the fluorophore increases during UV irradiation. This result is in accordance with our proposed model and is in contrast to the traditional luminescent core growth model. Such a short lifetime agrees with previous reports in Ag NCs and contrasts with the microsecond long lifetime observed in the Au NCs.[16,19,22]

The oligomeric Ag(I)-carboxylate complexes in the resulting solution were not luminescent under UV light prior to UV radiation (curve a in Figure 1b). Thus, we preclude the possibility of photoemission of oligomeric Ag(I)-carboxylate complexes. Nevertheless, the presence of a broad peak centered at 450 nm indicates that the emission from the Ag-carboxylate NCs could be attributed to LMCT from the oxygen atom in the carboxylate ligands to the Ag(I) ions on the surface of Ag NCs. Interestingly, the Ag(I)-carboxylate NCs could emit via a wide range of excitation wavelength. As shown in Figure 2a, fluorescence could be observed upon excitation between 410 and 630 nm. The emission maximum is excitation wavelength dependent, which has also been observed in other Ag NCs.[9,21] We attribute this phenomenon to the strong coupling between the surface plasmon and emitter in Ag NCs, which has been thoroughly studied in gold and silver films with thickness of tens of nanometers in Kretschmann geometry.[28−31] When strong coupling between surface plasmon and emitters exists, the resulting new energy states are

$$E_{U,L}(\lambda) = [E_{pl}(\lambda) + E_0]/2 \pm \sqrt{\Delta^2 + [E_{pl}(\lambda) + E_0]^2/4}$$

dx.doi.org/10.1021/ja407911b | J. Am. Chem. Soc. 2014, 136, 1686−1689

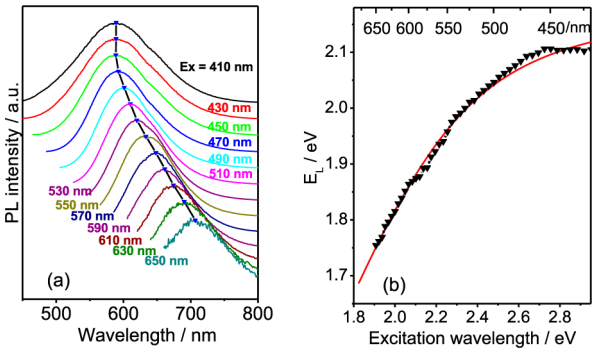

Figure 2. Strong coupling between the surface plasmon and the emitter in Ag-carboxylate NCs prepared using PMAA as a scaffold: (a) Emission spectra vs excitation wavelength and (b) emission peak positions (E_L) vs the excitation wavelength. Solid triangles indicate the experimental data, and the solid curve represents the theoretical simulation of the strong coupling model. The excitation wavelengths are indicated by Ex.

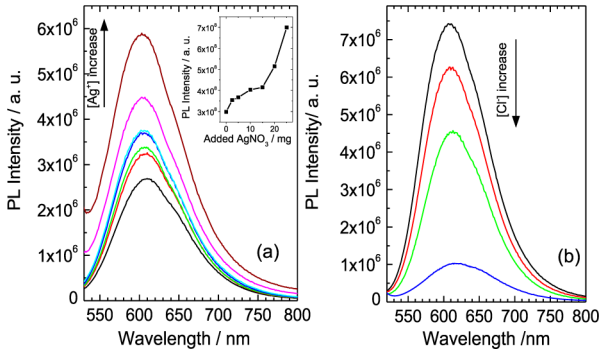

Figure 3. Luminescence enhancement and quenching by addition of (a) $Ag^+$and (b) Cl^- into the aqueous Ag-carboxylate NC solutions. The initial molar ratio of carboxylate/Ag^+ in (a) and (b) are 8:1 and 4:1, respectively. Inset in (a) displays the relationship between PL intensity and added $AgNO_3$.

where $E_{U,L}$ are the upper and lower energy, corresponding to the emission peaks, $E_{pl}(\lambda)$ is the noninteracting surface plasmon energy, λ is the wavelength of excitation light, E_0 is the energy related to emitter, and Δ is the energy related to the interaction between surface plasmons and emitters. We have changed the surface plasmon frequency by changing the frequency of excitation light, which is always in resonance with surface plasmons. The noninteracting surface plasmon energy thus is $E_{pl} = 1240/\lambda$, with E_{pl} in eV and λ in nm. Figure 2b presents the relationship between the excitation wavelength and emission peak. The solid line shows the lower energy E_L at $E_0 = 2.20$ eV and $\Delta = 266$ meV. The experimental emission peak curve overlaps with the theoretical curve predicted by the strong coupling model. Strong coupling damps the fluorescence and explains the short lifetime (1 ns) and low QY (4.6%) of our Ag-carboxylate NCs. Suppressing the plasmonic effects could probably enhance the QY of Ag-carboxylate NCs.

The high content of Ag(I)-carboxylate complexes in the shell of the luminescent Ag-carboxylate NCs was confirmed by XPS (Figure s7), and the proposed Ag(0)NCs@Ag(I)-carboxylate complex core−shell structural model is illustrated in Figure 1c. Most importantly, the XPS spectra showed the presence of an Ag oxidation state in the luminescent Ag-carboxylate NCs. The binding energy (BE) of the electron on the Ag $3d_{5/2}$ orbitals of the fluorescent Ag NCs can be deconstructed into Ag(I) and Ag(0) components with binding energies of 369.8 (∼30%) and 368.2 eV (∼70%), respectively.

When the principal absorption peak was tuned from 435 to 505 nm, both the PL intensity (Figure s3) and the percentage of Ag (I) in the Ag NCs shown by XPS are increased (see Figure s7a,b and Table s2). This suggests that the fluorescence is related to the Ag(I)-carboxylate complex shell. To further verify the validity of our model we modified the fluorescence signal of as-made Ag NCs solutions by dosing with Ag^+ cations, Cl^- anions, and diluted H_2O_2 solution.

In Figure 3a, with increasing amounts of $AgNO_3$, the PL intensity monotonically increases. However, when the chloride (Cl^-) anions with strong capacity to precipitate Ag(I) were incorporated, the luminescence was quenched. Decreasing emission of the Ag NCs is due to removal of the Ag^+ cations on the shell of Ag(I)-carboxylate complex in the Ag NCs. Similar results were reported by Pradeep, when cyanide and ammonia were added to the aqueous Ag_7 and Ag_8 NCs solution.[8] This strong complex ability of the Ag^+ also explains why the Ag NCs have useful detective capacity for amino acids with thiolate groups.[32] This experiment proved that the surface complex Ag^+ ions are a key component of the core−shell structure model.

To verify the oxygen etching effect on the Ag core during long-term storage, the H_2O_2 etching reaction was designed to prove that the increase of surface Ag^+ can enhance the photoluminescence of Ag NCs. With increasing H_2O_2 amounts added into the as-made Ag NCs solution, the intensity of absorption band centered at 435 nm was dramatically decreased, and concomitantly a new shoulder band centered at 500 nm appeared (Figure s8a), consistent with the results of samples stored at varied times (Figure s3). As expected, the intensity of PL centered at 600 nm significantly increased due to the increase of Ag^+ adsorbed on the core (Figure s8b). This further confirms that the surface complex Ag^+ ions play a paramount role in the tuning of photoluminescence emission in our core−shell structure model.

The type of surface ligands was another critical synthesis parameter with impact on the photoluminescence of Ag NCs. When the surface anchoring ligands were replaced by poly(sodium-4-styrenesulfonate) free of carboxylate groups, the Ag NCs did not show any photoluminescence even though the sizes are similar (Figures s2 and s9). However, when the poly(methyl vinyl ether-*alt*-maleic acid) (PMVEM, M_W = 80000−216000) with the same anchoring ligand as PMAA (M_W = 9000) was used as the surface anchoring ligand, the Ag NCs exhibited similar optical properties as Ag NCs synthesized using PMAA. The wavelength of both absorption and luminescence was blue-shifted due to size effects as seen in Figure 4a,b. TEM analysis showed that the new Ag NCs have a smaller particle size of ∼2.7 nm (Figure 4c) versus Ag NCs using PMAA as scaffolds.

Luminescence decay data confirmed the predominance of picosecond lifetime components in the Ag NCs: 0.14 ns (80%), 0.66 ns (18%), and 2.42 ns (1.9%) upon excitation at 420 nm. Such short lifetime is probably due to the strong coupling of surface plasmon and emitter in Ag-carboxylate NCs. Thus, the photoemission of the Ag NCs shows both high selectivity on the surface anchoring ligands and strong dependence on the particle size. Ag NCs with various DNA scaffolds have also been reported.[13,22−27] The N atom in DNA bases is also electron rich, and the LMMCT from N to silver could be the photoemission mechanism in the Ag NCs prepared with DNA scaffolds. Addition of electron-donating groups to organic scaffolds could be expected to give better photoluminescence properties in Ag NCs, similar to the Au NCs.[16]

dx.doi.org/10.1021/ja407911b | J. Am. Chem. Soc. 2014, 136, 1686−1689

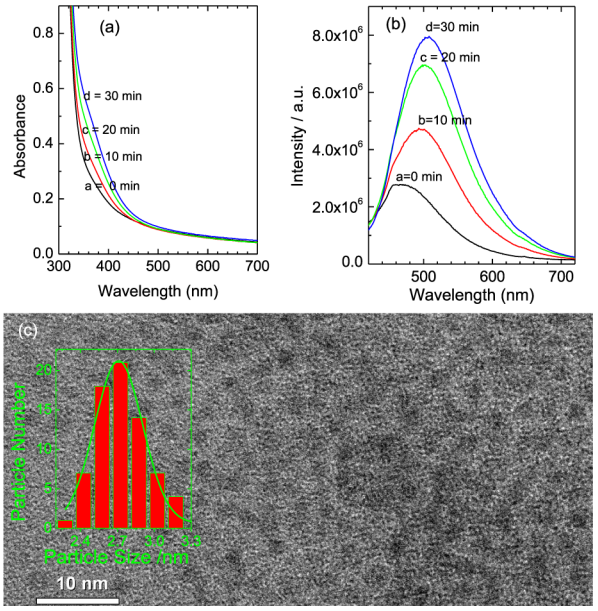

Figure 4. (a) Absorption and (b) emission spectra of Ag NCs prepared with PMVEM scaffold under UV photoreduction and (c) HR-TEM image of Ag NCs. Histograms describe the statistical distribution of particle size; the particle size is ~2.7 nm. The COO^-/Ag^+ molar ratio used for the synthesis was 4:1.

In summary, we studied the photoemission mechanism of 2−5 nm Ag-carboxylate NCs. The origin of photoluminescence from Ag NCs cannot be simply attributed to the discrete Fermi energy levels in the Ag NCs. Solid experimental evidence shows that the photoemission in Ag NCs highly depends on the LMMCT from Ag(I)-carboxylate complexes to the Ag atoms. The emission of Ag NCs is strongly dependent on the amount of surface Ag^+, the type of surface anchoring ligands, and the particle size. Remarkably, when the Ag(0) core is large enough (even in 2−5 nm) to support plasmonic resonance, strong coupling of the surface plasmon and the emitter in Ag-carboxylate NCs occurs. This alters the optical properties of Ag NCs, including their short lifetime, relatively low QY, and absorption and emission peak positions. Overall, our studies clarify the emission mechanism of Ag NCs, a step pivotal to the design and synthesis of highly luminescent Ag or Au NCs.

■ ASSOCIATED CONTENT

Supporting Information

Synthesis and characterization details.This material is available free of charge via the Internet at http://pubs.acs.org.

■ AUTHOR INFORMATION

Corresponding Authors

kzhang@chem.ecnu.edu.cn
sjzhang@phy.ecnu.edu.cn

Author Contributions

§These authors contributed equally.

Notes

The authors declare no competing financial interest.

■ ACKNOWLEDGMENTS

The authors thank Prof. Zhenrong Sun for helpful discussions about nanocluster photophysics, and also appreciate Dr. Ting Wu, Dr. E Wu, and Mrs. Ming Song for their assistances in the XPS, coupled AFM, and fluorescence imaging characterizations, respectively. This work is supported by the National Science Foundation of China (21003050, 61008003, 21373004, and 20925310), the Science and Technology Commission of Shanghai (10ZR1410500, 08DZ2273300, 11QA1402100, 10PJ1403200), the Ph.D. Programs Foundation of the Ministry of Education of China (20100076120019), the Shanghai Municipal Education Commission and Shanghai Education Development Foundation (12ZZ037, 11CG24), the Fundamental Research Funds for the Central Universities, and JoRRIS project.

■ REFERENCES

(1) Jin, R. *Nanoscale* **2010**, *2*, 343.
(2) Zheng, J.; Nicovich, P. R.; Dickson, R. M. *Annu. Rev. Phys. Chem.* **2007**, *58*, 409.
(3) Diez, I.; Ras, R. H. *Nanoscale* **2011**, *3*, 1963.
(4) Yuan, X.; Luo, Z. T.; Zhang, Q. B.; Zhang, X. H.; Zheng, Y. G.; Lee, J. Y.; Xie, J. P. *ACS Nano* **2011**, *5*, 8800.
(5) Lu, Y.; Chen, W. *Chem. Soc. Rev.* **2012**, *41*, 3594.
(6) Wilcoxon, J. P.; Abrams, B. L. *Chem. Soc. Rev.* **2006**, *35*, 1162.
(7) Aherne, D.; Ledwith, D. M.; Gara, M.; Kelly, J. M. *Adv. Funct. Mater.* **2008**, *18*, 2005.
(8) Rao, T. U. B.; Pradeep, T. *Angew. Chem., Int. Ed.* **2010**, *49*, 3925.
(9) Xu, H.; Suslick, K. S. *ACS Nano* **2010**, *4*, 3209.
(10) Shen, Z.; Duan, H.; Frey, H. *Adv. Mater.* **2007**, *19*, 349.
(11) Zhang, J. G.; Xu, S. Q.; Kumacheva, E. *Adv. Mater.* **2005**, *17*, 2336.
(12) Diez, I.; Pusa, M.; Kulmala, S.; Jiang, H.; Walther, A.; Goldmann, A. S.; Muller, A. H. E.; Ikkala, O.; Ras, R. H. A. *Angew. Chem., Int. Ed.* **2009**, *48*, 2122.
(13) Pal, S.; Varghese, R.; Deng, Z. T.; Zhao, Z.; Kumar, A.; Yan, H.; Liu, Y. *Angew. Chem., Int. Ed.* **2011**, *50*, 4176.
(14) Yuan, X.; Setyawati, M. I.; Tan, A. S.; Ong, C. N.; Leong, D. T.; Xie, J. P. *NPG Asia Mater.* **2013**, 5.
(15) Zheng, J.; Ding, Y.; Tian, B.; Wang, Z. L.; Zhuang, X. *J. Am. Chem. Soc.* **2008**, *130*, 10472.
(16) Wu, Z.; Jin, R. *Nano Lett.* **2010**, *10*, 2568.
(17) Luo, Z.; Yuan, X.; Yu, Y.; Zhang, Q.; Leong, D. T.; Lee, J. Y.; Xie, J. *J. Am. Chem. Soc.* **2012**, *134*, 16662.
(18) Huber, K.; Witte, T.; Hollmann, J.; Keuker-Baumann, S. *J. Am. Chem. Soc.* **2007**, *129*, 1089.
(19) Shang, L.; Dong, S. *Chem. Commun.* **2008**, 1088.
(20) Wang, X. M.; Xu, S. P.; Xu, W. Q. *Nanoscale* **2011**, *3*, 4670.
(21) Diez, I.; Kanyuk, M. I.; Demchenko, A. P.; Walther, A.; Jiang, H.; Ikkala, O.; Ras, R. H. A. *Nanoscale* **2012**, *4*, 4434.
(22) Vosch, T.; Antoku, Y.; Hsiang, J.-C.; Richards, C. I.; Gonzalez, J. I.; Dickson, R. M. *Proc. Natl. Acad. Sci. U.S.A.* **2007**, *104*, 12616.
(23) Sharma, J.; Yeh, H.-C.; Yoo, H.; Werner, J. H.; Martinez, J. S. *Chem. Commun.* **2010**, *46*, 3280.
(24) Petty, J. T.; Zheng, J.; Hud, N. V.; Dickson, R. M. *J. Am. Chem. Soc.* **2004**, *126*, 5207.
(25) Gwinn, E. G.; O'Neill, P.; Guerrero, A. J.; Bouwmeester, D.; Fygenson, D. K. *Adv. Mater.* **2008**, *20*, 279.
(26) Xu, H.; Suslick, K. S. *Adv. Mater.* **2010**, *22*, 1078.
(27) Feng, L.; Huang, Z.; Ren, J.; Qu, X. *Nucleic Acids Res.* **2012**, *40*, e122.
(28) Bellessa, J.; Bonnand, C.; Plenet, J. C.; Mugnier, J. *Phys. Rev. Lett.* **2004**, *93*, 036404.
(29) Salomon, A.; Gordon, R. J.; Prior, Y.; Seideman, T.; Sukharev, M. *Phys. Rev. Lett.* **2012**, *109*, 073002.
(30) Berrier, A.; Cools, R.; Arnold, C.; Offermans, P.; Crego-Calama, M.; Brongersma, S. H.; Gomez-Rivas, J. *ACS Nano* **2011**, *5*, 6226.
(31) Gomez, D. E.; Vernon, K. C.; Mulvaney, P.; Davis, T. J. *Nano Lett.* **2010**, *10*, 274.
(32) Shang, L.; Dong, S. J. *Biosens. Bioelectron.* **2009**, *24*, 1569.